RADIOFREQUENCY ABLATION WITH TWO SODIUM CHLORIDE CONCENTRATIONS COOLING SOLUTIONS AND ITS INFLUENCE ON DOG THIGH MUSCLE TISSUE DAMAGE CHARACTER AND SIZE

Gintautas Vaitiekaitis[1], Aleksandras Vitkus[2], Algis Noreika[3], Ingrida Balnytė[2], Alius Pockevičius[4], Neringa Balčiūnienė[5], Julius Liobikas[6], Danas Baniulis[7], Aldona Gružienė[8]
[1]Department of Physics Mathematics and Biophysics, Medical Academy, Lithuanian University of Health Sciences A. Mickevičiaus Str. 9, Kaunas, Lithuania, LT-44307
e-mail vaitiekaitis@vision.kmu.lt, tel. (+370 37) 327367, fax. (+370 37) 220733
[2]Department of Histology and Embryology, Lithuanian University of Health Sciences
e-mail avitkus@gmail.com, tel. (+370 37) 327315, e-mail angval@kmu.lt, tel. (+370 37) 327236
[3]Department of Noninfectious Diseases, Veterinary Academy, University of Health Sciences
Tilžės Str. 18, Kaunas, Lithuania, LT-47181, e-mail algis.noreika@lva.lt, tel. (+370 37) 409741
[4]Department of Infectious Diseases, Veterinary Academy, LUHS; e-mail palius@lva.lt, tel. (+370 37) 409740
[5]Department of Intensive Care, Neurosurgery Intensive Care Unit
Hospital of Lithuanian University of Health Sciences "Kauno Klinikos"
Eivenių Str. 2, Kaunas, Lithuania, LT-50009
e-mail xnerisx@gmail.com, tel. (+370 37) 327104
[6]Institute of Neurosciences, Laboratory of Biochemistry, Medical Academy, LUHS
Eivenių Str. 4, Kaunas, Lithuania, LT-44307; e-mail julius.liobikas@bioch.eu, tel. (+370 37) 302968
[7]Department of Genetic and Biotechnology of Orchard Plants, Institute of Horticulture, Lithuanian Center for Agriculture and Forestry
Kauno Str. 30, Babtai, Kaunas Distr., Lithuania, LT-54333; e-mail d.baniulis@lsdi.lt, tel. (+370 37) 555233
[8]Institute of Physiology and Pharmacology, Lithuanian University of Health Sciences
A. Mickevičiaus Str. 9, Kaunas, Lithuania, LT-44307; e-mail aldona.gruziene@kmu.lt, tel. (+370 37) 327256.

Abstract. During the last decades, one of the most common nondrug therapies used for patients cardiac arrhythmia treatment is a controlled thermal destruction of certain myocardial structures and tissues. However, the investigations of small microstructural changes of thermal tissue destruction are neglected. This study investigated the effect of radiofrequency ablation with active electrode cooling, on dog thigh muscle damage character and size. Three experiment sessions were performed on thirteen mongrel dogs. The first radiofrequency ablation session was done without cooling. In the second session the electrode was cooled with a 0.1% NaCl solution and during the third session, cooling was made with a 0.9% NaCl solution. In all cases the duration of ablation was 30 s and the power was 40 W. Lastly, the calculations of a theoretical model were accomplished. Our experimental results show that the strongest impact of the ablation on tissue damage was observed in the first session, medium in the second session and the lowest in the third session. The average damaged area of ablated tissue was the largest in the first session, medium in the third session and the smallest in the second session ($p<0.05$). The highest temperature on the surface of the heated tissues at the ablating electrode contact site during the ablation procedure was measured in the first session, medium in the second session and smallest in the third session. Experimental results and theoretical calculations allow making an assumption that the different concentrations of cooling solution influence the ablating tissue damage size and character, due to the redistribution of electric field strength lines. The examination of histological preparations revealed that in the tissues affected by the ablation procedure the enclosed „ring" shape stripe of damaged area is detectable.

Keywords: cardiac arrhythmia, radiofrequency ablation, cooling solution, thermal tissue damage.

RADIODAŽNUMINĖS ABLIACIJOS ĮTAKA ŠUNS ŠLAUNIES RAUMENS AUDINIŲ PAŽEIDIMO POBŪDŽIUI IR MASTUI, KAI AUŠINIMUI TAIKOMI DU SKIRTINGOS KONCENTRACIJOS NATRIO CHLORIDO TIRPALAI

Gintautas Vaitiekaitis[1], Aleksandras Vitkus[2], Algis Noreika[3], Ingrida Balnytė[2], Alius Pockevičius[4], Neringa Balčiūnienė[5], Julius Liobikas[6], Danas Baniulis[7], Aldona Gružienė[8]
[1]Fizikos, matematikos ir biofizikos katedra, Medicinos akademija, LSMU
A. Mickevičiaus g. 9, Kaunas, LT-44307; tel. (+370 37) 32 73 67; faks. (+370 37) 22 07 33
el. paštas: vaitiekaitis@vision.kmu.lt
[2]Histologijos ir embriologijos katedra, Medicinos akademija, LSMU
A. Mickevičiaus g. 9, Kaunas, LT-44307; tel. (+370 37) 32 73 15; el. paštas: avitkus@gmail.com; angval@kmu.lt
[3]Neužkrečiamųjų ligų katedra, Veterinarijos akademija, LSMU
Tilžės g. 18, Kaunas, LT-47181; tel. (+370 37) 40 97 41; el. paštas: algis.noreika@lva.lt
[4]Užkrečiamųjų ligų katedra, Veterinarijos akademija, LSMU
Tilžės g. 18, Kaunas, LT-47181; tel. (+370 37) 40 97 40; el. paštas: palius@lva.lt

[5]*Neurochirurgijos intensyviosios terapijos skyrius, Intensyviosios terapijos klinika, LSMU ligoninė Kauno klinikos*
Eivenių g. 2, Kaunas, LT-50009; tel. (+370 37) 32 71 04; el. paštas: xnerisx@gmail.com
[6]*Biochemijos laboratorija, Neuromokslų institutas, Medicinos akademija, LSMU*
Eivenių g. 4, Kaunas, LT-44307; tel. (+370 37) 30 29 68; el. paštas: julius.liobikas@bioch.eu
[7]*Sodo augalų genetikos ir biotechnologijos skyrius, Lietuvos agrarinių ir miškų mokslų centro filialas*
Sodininkystės ir daržininkystės institutas
Kauno g. 30, Babtai, Kauno r., LT-54333; tel. (+370 37) 55 52 33; el. paštas: d.baniulis@lsdi.lt
[8]*Fiziologijos ir farmakologijos institutas, Medicinos akademija, LSMU*
A. Mickevičiaus g. 9, Kaunas, LT-44307; tel. (+370 37) 32 72 56; el. paštas: aldona.gruziene@kmu.lt

Santrauka. Pastaraisiais dešimtmečiais vienas labiausiai paplitusių pacientų širdies aritmijų nemedikamentinio gydymo būdų yra terminė tam tikrų miokardo struktūrų ir audinių destrukcija. Tačiau atlikta nedaug tyrimų, kur būtų nagrinėta maži mikrostruktūriniai pokyčiai, atsiradę po terminės audinių destrukcijos. Šiuo darbu tyrėme radiodažnuminės abliacijos poveikį šuns šlaunies skersaruožio raumens pažeidimo mastui ir pobūdžiui, kai abliacinis elektrodas yra aktyviai aušinamas. Tyrimams naudota trylika negrynaveislių šunų. Atliktos trys bandymų serijos. Pirmosios metu radiodažnuminė abliacija atlikta neaušinant abliacinio elektrodo. Antruoju bandymu abliacinis elektrodas buvo aušinamas 0,1 proc. NaCl tirpalu, o trečiuoju – 0,9 proc. NaCl tirpalu. Visais atvejais abliacija truko 30 s, o abliacijos galingumas buvo 40 W. Taip pat atlikti teorinio modelio skaičiavimai. Mūsų bandymų rezultatai parodė, kad abliacijos poveikis audinių terminiam pažeidimui stipriausias buvo pirmosios bandymų serijos metu, vidutinis – antrosios ir silpniausias – trečiosios. Didžiausias abliuotų audinių pažeidimo ploto vidurkis nustatytas pirmosios eksperimentinės serijos metu, vidutinis – trečiosios ir mažiausias – antrosios ($p<0,05$). Per pirmąją bandymų seriją abliacijos procedūros metu elektrodo kontakto su kaitinamais audiniais vietoje paviršiaus temperatūra buvo didžiausia, vidutinė temperatūra buvo antrosios bandymų serijos metu ir mažiausia – trečiosios. Tyrimų rezultatai ir teoriniai skaičiavimai leido daryti prielaidą, kad skirtingos koncentracijos aušinimo tirpalai perskirsto elektrinio lauko jėgos linijų išsidėstymą aplinkoje ir dėl to daro įtaką abliuojamų audinių pažeidimo pobūdžiui ir mastui. Ištyrę histologinius preparatus nustatėme, kad audiniuose, pažeistuose radiodažnuminės abliacijos metodu, matyti uždaras „žiedo“ formos pažeidimas.

Raktažodžiai: širdies aritmija, radiodažnuminė abliacija, aušinimo tirpalas, terminis audinių pažeidimas.

Introduction. During the last decades, cardiovascular disease has been recognized as one of the most common diseases among human population (Jongbloed M.R.M. 2010, Nattel S. 2002). It is noteworthy, that various forms of arrhythmias, for a number of reasons, cause most of cardiovascular diseases (Jongbloed M.R.M. 2010, Nattel S. 2002). In particular, atrial fibrillation is one of the most common forms of arrhythmia (Nattel S. 2002). Atrial fibrillation (AF) can be caused by severe diseases, such as coronary artery disease, pericardits, mitral valve disease, congenital heart disease, congestive heart failure, thyrotoxic heart disease and hypertension (Nattel S. 2002). Mostly, AF develops in patients and increases in population with age: from 0.5% in people 50 years of age and over, and up to 10% in people 80 years old in the most developed countries (Nattel S. 2002). Obviously, AF and cardiovascular diseases are of a systematic nature among this group of people. Such diseases mostly become chronic and usually cause a long-term atrial arrhythmias, which reduce the quality of their life (Nattel S. 2002). The patients, whose arrhythmias can not be treated effectively with drugs, usually receive other types of treatment (Jongbloed M.R.M. 2010, Organ L.W. 1976-1977, Nattel S. 1998, Oral H. 2007, Calkins H. 2009).

One of the most common nondrug therapies used for cardiac arrhythmia treatment is a controlled thermal destruction of certain myocardial structures and tissues, which might generate arrhythmias (Jongbloed M.R.M. 2010, Ware D.L. 1999, Petersen H.H. 2004, Yokoyama K. 2006, 2009). This treatment method is reasoned as myocardial heating and is easily achievable by transcatheter radiofrequency energy delivery. Furthermore, it has been demonstrated to be an effective and technically simple means of making the focal myocardial thermal injury (Cosman E.R. 1988, Nakagawa H. 1995, Nakagawa H.1998). Since the cardiac conduction paths and other anatomical structures are of a complex morphology, the distances between them are small and vary a dozen or a few millimeters within the limits (Jongbloed M.R.M. 2010, Güden M. 2002, Filho C.A., 2005). Consequently, it is important to know the size and the severity of the violations that will be caused by myocardial destruction of controlled thermal treatment (Jongbloed M.R.M. 2010, Güden M. 2002, Filho C.A., 2005). In most cases, thermal myocardial destruction is achieved by cooling ablative electrode with various cooling solutions, which are intended to protect against thrombi formation in cardiac chambers (Cerecedo D. 2006). It is well known and widely investigated that the concentration and the temperature of cooling solutions affect the change of the lesion size and the damage strength formation in myocardium (Petersen H.H. 1999, Bunch T.J. 2005, Stagegaard N. 2005). However, the investigation of radiofrequency (RF) ablation effects on tissue damages mostly resulted in the determination and analysis of heated tissue macrodestruction and their influence on the cardiac conductive system, contractile efficacy function or cardiovascular system (Filho C.A., 2005). The investigations of small microstructural changes of thermal tissue destruction are neglected. For

instance, one of the most recent analysis, of heated tissue macrodestruction and damaged tissues microstructural characters after RF ablation was published by scientists Weiss, Stiuart et al. in 2004.

It is noteworthy, that the nature of microstructural thermal tissue damage and its small variations could be important when the cooling RF ablation destruction of cardiac conduction system is accomplished. Such small tissue damage variations can be best studied on the dog thigh muscle tissue, because its structural properties are close to the myocardium (Weiss C. 2004). Also experiments on dog thigh muscle allow researchers to ensure constant contact between ablation electrode and muscle surface through the RF ablation procedure (Yokoyama K. 2006, Nakagawa H. 1995, Nakagawa H. 1998).

Because of all the above, the purpose of this study was to investigate the size and nature of tissue thermal damage caused by the cooling RF ablation, when 0.1% and 0.9% sodium chloride solutions were used to cool the ablative electrode.

Materials and methods. The experimental protocol was taken from scientific papers of researchers Nakagawa, Yokoyama and co-authors, published in 1995-2006 years. The eperiments were carried out in accordance to Lithuanian animal care, management and use legislation No.8-500 (State news, 28 November 1997, No.108) and EU Directive 86/609/EEC and EC recommendations 2007/526 EC "Using and keeping of animals for experimental and other purposes". Thirteen mongrel dogs, weighting between 26 and 40 kg were anesthetized with midazolam (bolus, 25 mg; infusion, 3 to 6 mg/h) and ketamine (bolus, 750 mg; infusion, 100 to 200 mg/h) (Nakagawa H. 1998). Initially, after the injection of anaesthetic agents into the back of dogs' thigh, a 15 cm skin incision was made on the right or left thigh. Subsequently, the muscle was uncovered and the skin was shaped to form a cradle (Yokoyama K. 2006, Nakagawa H. 1995). A typical ablation catheter with a 2 mm diameter tip electrode was used in this study (Yokoyama K. 2006, Nakagawa H. 1995, Nakagawa H. 1998, Moulton L. 2003). The ablation catheter was inserted into a thin pipe for irrigation (Moulton L. 2003). A thermocouple electrode was used to measure the temperature at the ablation site (Yokoyama K. 2006, Nakagawa H. 1995, Nakagawa H. 1998). Both ablation and thermocouple electrodes were positioned perpendicular to the thigh muscle during all the experiments. At first, the tip of the ablation electrode was driven up to the tissue surface and then it was pushed with constant weight of 10 g. (Yokoyama K. 2006, Nakagawa H. 1998). After that, the thermocouple electrode tip was driven up to the tissue surface and bundled up with the ablation electrode. The cooling solution was administered to the ablation site at the rate of 16 ml/min during ablation procedure (Yokoyama K. 2006, Nakagawa H. 1995, Nakagawa H. 1998). Sodium chloride (NaCl) solution irrigation was initiated at the same moment as the RF ablation started and was maintained until RF application stopped. The concentrations of NaCl cooling solutions were 0.1% and 0.9%. We chose such concentrations of NaCl because these are mostly used in clinical practice**.** The temperature of the cooling solutions was 20 ^{o}C. The duration of RF ablation procedure was 30 s. Ablation power of 40 W (500 kHz) was delivered at a constant voltage mode. During the procedure, the resistance varied in the range from 110 to 210 Ω (Yokoyama K. 2006, Nakagawa H. 1995, Nakagawa H. 1998). Energy of RF ablation was delivered between the ablation electrode and adhesive electrosurgical dispersive pad applied to the shaved opposite side of the thigh (Nakagawa H. 1995). During each RF application, changes of impedance and temperature on tissue surface were monitored. RF ablation was performed in three different places on the *Musculus quadriceps femoris* surfaces of right and left legs for each dog.

In total, three various ablation sessions took place. The first experimental ablation session was done without cooling of RF ablation electrode (no cooling – NC). During the second experimental session the electrode was cooled with a 0.1% NaCl solution (cooling with 0.1% NaCl – C0.1) and during the third experimental session the electrode was cooled with a 0.9% NaCl solution (cooling with 0.9% NaCl – C0.9).

After the last RF ablation procedure, each dog was euthanized 4–6 hours later and the experiment was finished (Nakagawa H. 1998, Wittkampf F.H. 1996). Afterwards, the tissue specimens with necrosis were taken and then fixed in 10% formalin solution.

After each experimental session, all tissue specimens were sectioned into a number of slices. After NC experimental session 19 slices per specimen were sectioned, after C0.9 session 20 slices per specimen and after C0.1 session 23 slices were prepared per specimen. Histological preparations of damaged tissues were done in the following way. Paraffine embedded sections were sliced with a microtome (step 0.2-0.3 mm), mounted on slides and stained with hematoxylin and eosin (Weiss C. 2004). Then, the necrosis area was identified and measured in each histological slice, as well as the relative strength and the character of the tissue damages were evaluated (Ware D.L. 1999, Nakagawa H. 1998, Weiss C. 2004, Wittkampf F.H. 1996).

Micrographs of histological preparations were taken with computerized microscope OLYMPUS BX 40. Measurements and analyses of histological photographs were made with software ImageJ, Microvision 1.1 and Cell Sens Dimensions 2010. All data are expressed as mean ± standard error.

The calculation of theoretical model (Tatur T.A. 1989, Tungjitkusolmun S. 2000, Bhavaraju N.C. 1999) of ablation electrode electric field distribution in tissues was performed by adapting the mirror reflection method (Tatur T.A. 1989).

Results. Our experiments showed that during the RF ablation procedure different cooling conditions of ablation electrode resulted in different temperatures on the tissue surface around ablation electrode. These conditions also resulted in different impedances in ablation electrode contact site with tissues. In the NC session of experiments

(ablation electrode no cooling), the average impedance during the ablation procedure was 110±3.6 Ω, and the temperature on the tissue surface in contact site ranged from 31 to 32 ºC. In the C0.1 session of experiments (ablation electrode cooling with 0.1% NaCl solution), the average impedance was 140±5.6 Ω. During this experimental session, the temperature on the tissue surface in ablation electrode contact site, during the ablation procedure ranged from 26 to 30.4 ºC. It is noteworthy, that the temperature was 0.6 - 6 ºC lower in comparison with the NC session ($p<0.05$). In the C0.9 experimental session (ablation electrode cooling with 0.9% NaCl solution), the average impedance was 100±1.6 Ω, whereas the temperature on the tissue surface during the procedure ranged from 20 to 25.4 ºC. During this experimental session the temperature was 5.6 - 12 ºC lower in comparison with the NC session ($p<0.05$).

The analysis of histological preparations showed that the greatest damage of tissues after RF ablation was observed in the NC experimental session, while the smallest damage of tissues were observed in the C0.9 experimental session. Importantly, despite different experimental conditions during all three RF ablation experimental sessions, several clearly defined damage zones of tissues were identified. These zones are possible to be differentiated by character and size of tissue damage. The main damaged zones of tissues, which were formed after RF ablation, are presented in Fig. 1.

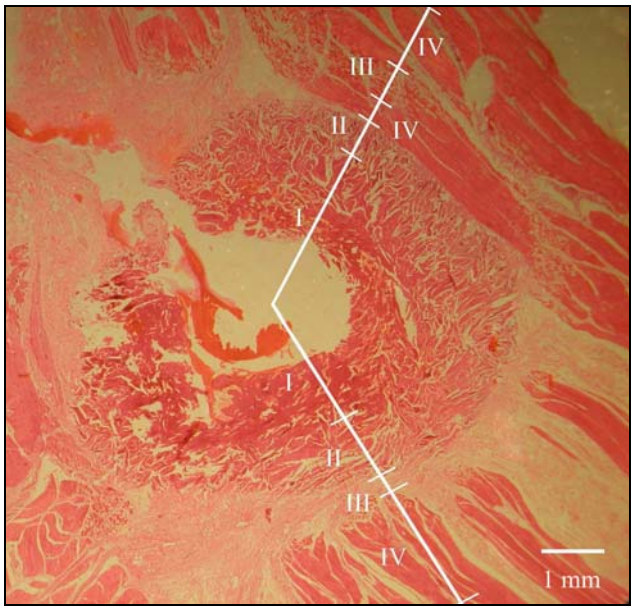

Fig.1. **This figure presents a typical histological view of canine thigh tissues after the ablation procedure** (experimental session C0.1) **with four damage zones:** I – carbonization tissues; II – unstructured non-nucleated mass of damaged tissues**,** destroyed myocytes and stromal edema; III – coagulative myolysis, autolysed myofibrils, these myofibrils appear as small lumps; IV – segmental hypercontraction of myocytes and the coagulative myolysis. The histological view presented in this figure is magnified by x40 times.

The first damage zone (Fig.1. I) is characterised by charred and carbonized tissue, which is morphologically visible in histological preparations. This zone generally coincides with the contact site of the ablation electrode and such damages are caused by direct mechanical and thermal effects on tissues surrounding the electrode tip. Mostly, during the preparation of histological slices, such seriously damaged tissues fall off to form blank areas in the histological slice (Fig.1. I).

The second damage zone (Fig. 1. II) is characterised by coagulative necrosis and is observed in the surface layers of necrotic tissues at a depth of 1–2 mm from the ablation electrode tip and in the layers of damaged tissues located slightly deeper from the surface, usually 3–5 mm deep. The second damage zone is usually formed around the first (Fig.1. I, II). In the second zone, the unstructured non-nucleated mass of damaged tissues surrounded by hyperemic edge can be observed (Fig. 1. II).

The third damage zone (Fig.1. III) is either formed only around one outer side of the second damage zone or can be fully formed around the entire second zone. The third zone is characterized by coagulative myolysis. The outer edge of the third zone is formed by a striking but not very wide "ring" which consists of destroyed and autolysed myofibrils. In histological preparations these myofibrils appear as small lumps of various sizes (Fig. 1. III).

The fourth tissue damage zone (Fig. 1. IV) is characterized by segmental hypercontraction. It forms behind the third damage zone, but also often forms between the second and third tissue damage zones (Fig. 1. IV). It should be noted that, the tissue damage of the fourth zone are of smaller strength in comparison with the second or third zones damages. In the fourth tissue damage zone, segmental hypercontraction of myocytes and the coagulative myolysis of muscles presented alongside and are observed morphologically. In this zone fibres of damaged tissue are usually curved. Away from the fourth tissue damage zone, at the farthest distance from the ablation electrode contact site are undamaged tissues. These tissues compose intact zone and are not seen in the presented figures.

Comparing the severity of the tissue damage in all experimental sessions, we found that the strongest impact of the RF ablation on tissue damage was observed in the NC experimental session, the medium impact was observed in the C0.1 session and the lowest in the session C0.9.

In all the three experimental sessions, the visible average areas of damaged tissues of all histological specimens were as follows: in the NC experimental session, the average damaged area of necrotic lesion was 29.13 ± 9.02 mm^2; in the C0.9 experimental session, the average damaged area of necrotic lesion was 17.72 ± 2.62 mm^2; in the C0.1 experimental session, the average damaged area of necrotic lesion was 14.71 ± 1.96 mm^2. On comparing these results of all free experimental sessions it has been statistically significantly established ($p<0.05$) that the largest average area of coagulation necrosis was obtained in the NC experimental session, the

smaller in the C0.9 session and the smallest in the C0.1 session.

For better understanding of the real dimensions and characters of tissue damages after cooled RF ablation, in Fig. 2, we present the most typical histological specimen.

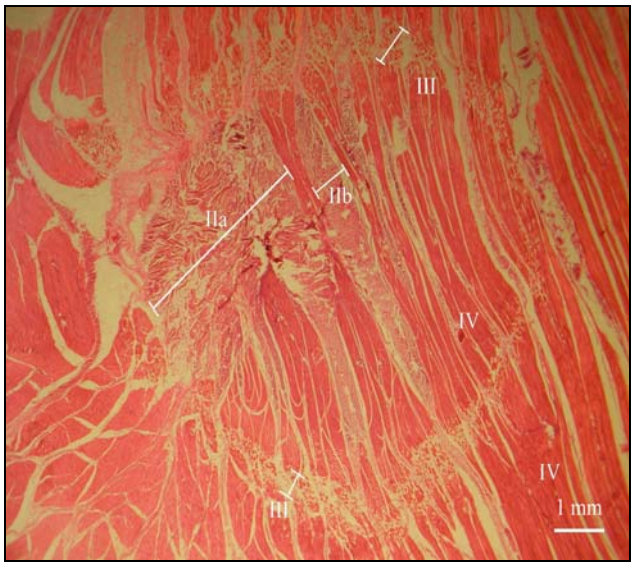

Fig. 2. **This figure shows the most typical canine thigh tissue damages after RF ablation in C0.1 experimental session.** Here, it is shown the ninth histological specimen, which was located at a depth of 3.6 mm from the tissue surface. In this figure, II, III and IV damage zones are seen magnified x40 times.

It was observed that the first damage zone is not visible in the central part of the presented histological view (Fig. 2.). This damage tissue zone is absent because the histological specimen was taken at a depth of 3.6 mm from the tissue surface, where the tissues is not in direct contact with the ablation electrode like the surface layers. Moving away from the centre of the histological specimen, which coincides with the place where the ablation electrode was positioned into the tissue, two fragments (Fig. 2. IIa., IIb.) of the second damage zone are visible. These fragments are like homogenous structures of the dark red tissues. A smaller damage fragment (Fig. 2. IIb.), 4.021±0.175 mm^2 in size, is of elliptical shape and it is directed parallel to all histological specimen fibres. In the upper left side of the specimen, a bigger fragment of the damage (Fig. 2. IIa.) 15.975±1,029 mm^2 in size and having an irregular shape is seen. It should be noted that in this histological specimen a narrow circular ″ring″ form the third damage zone is clearly visible (Fig. 2. III). This damage is made up of small fragments of the destroyed tissues. The area of this damage "ring" is 60.382±0.932 mm^2, the diameter in the longitudinal direction is 8.557±0.119 mm and in the transversal direction it is 8.288±0.179 mm.

It is important to note, that in some cases, the lower intensity fourth damage (Fig. 2. IV) or intact zones may be formed closer to the damage center, while the third damage zone (Fig. 2. III), having a stronger tissue damage, can be formed further.

Discussion. Analysis of obtained experimental results show that the average area of tissue damage does not always increase gradually with a tissue surface heating temperature augmentation at the electrode contact site, when ablation electrode is cooling with different concentrations of NaCl solutions. So, we make an assumption, that this phenomenon occurs because different concentrations of cooling solutions lead to a different distribution of electric field strength lines density in the heating tissues and the physical parameter like the heating temperature influences the formation of damage tissue character and areas.

Such an interesting phenomenon can be illustrated with a simple mathematical model of the electric field strength lines density distribution in two different environments. The results of theoretical calculations are shown in Figs 3a, 3b, and 3c.

In Fig. 3a, the theoretical distribution of the electric field strength lines of RF ablation in two ideal environments with the same electrical conductivity is shown

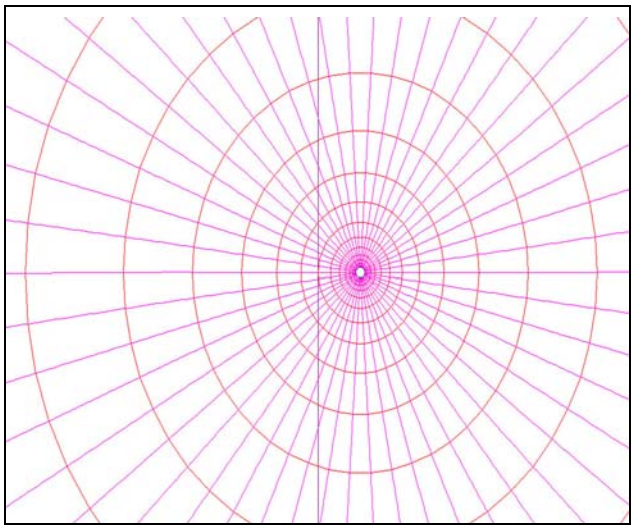

Fig. 3a. **A solid line in the middle of this picture shows the border between two ideal environments**

The tissue environment is located on the left side. In the right side, the environment of blood or cooling solution is located and there the ablation electrode is placed. Electrode localization refers to the circle and solid lines coming out of this circle represent the lines of electric field strength. Concentric circles around the electrode display equipotential surfaces of the electric field. In this case, the relative electrical conductivity of both environments is the same and is equal to 1 (γ=1). It should be noted, that relative electrical conductivity of ideal environments shows the ratio, which means how much, one environmental electrical conductivity is higher or lower than the other environment.

Secondly, in Fig. 3.b, theoretical calculation results, simulating situation in the C0.9 experimental session, are shown.

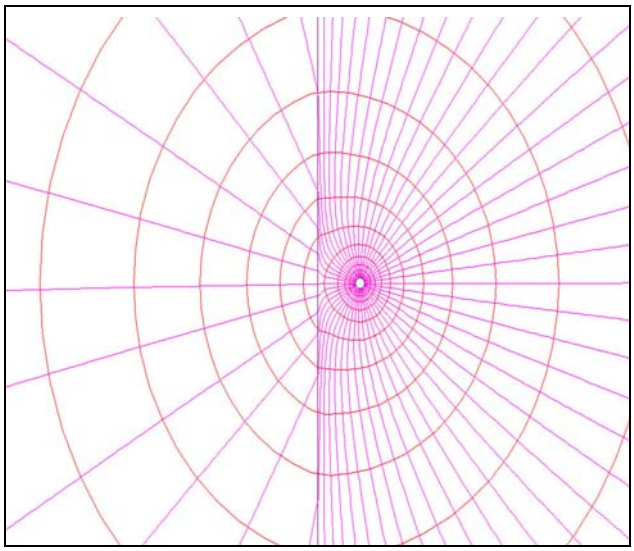

Fig. 3b. This **example shows the theoretical distribution of electric field strength lines of RF ablation through the border between two environments**

Tissues, whose electrical conductivity is more similar to the dielectric environment, are modelled on the left side of the board. The environment of the 0.9% NaCl cooling solution, whose dielectric properties are more similar to the conductor‘s environment, is modelled on the right side. On the right side, the relative electrical conductivity value is equal to 1, on the left side to 0.1.

As seen in Fig. 3b, the electric field strength lines exit from the electrode, then bend and thicken parallel to the border between both environments. The border is crossed by a relatively small number of electric field strength lines and behind the border in the environment, which reflects the tissue, density of lines is much less. This case of the model shows that the bigger part of the current flow parallels border surfaces, while smaller part of ablation current is passed to another environment. This means that these conditions lead to the ablating current shunting by cooling solution. This theoretical case (Fig. 3b.) is a proper modelling of the situation when the ablation electrode is introduced into the heart chambers and the ablation procedure is underway without cooling or with 0.9% NaCl cooling solution. Such modelling is usable, because blood and 0.9% NaCl cooling solution environments are similar and electrically both environments are like conductors. So, in this case of the model, the myocardial tissue electrical characteristics are chosen to be more similar to the dielectric ones, whereas blood and 0.9% NaCl cooling solution are chosen to be more similar to conductor environments.

In Fig. 3c, we present theoretical calculation results reflecting the experiment cases, where the ablation electrode is cooled by 0.1% NaCl solution.

Tissue environments are modelled on the left side of the border, whereas the environment of the 0.1% NaCl cooling solution is modelled on the right side. Electrical conductivity properties of the 0.1% NaCl solution environment are modelled much more similar to the dielectric environment. In this case on the left side of the border, the relative electrical conductivity value is equal to 1 and on the right side to 0.001.

It should be noted, that in this theoretical model, the ratio of both environments electrical conductivity was chosen in such a way, that 0.1% NaCl cooling solution environment was much more similar to the dielectric one than the tissues environment. Considering the calculation results presented in Fig. 3c, electric field strength lines of RF ablation exit from the ablation electrode and concentrate more around the electrode then they bend and cross the border of environments perpendicular to the border. It should be noted, that the density of electric field lines crossing the border between the two environments is higher near the electrode, and lower further away. Therefore, it is clear, that the bigger part of ablation current density will pass into the tissues near the electrode.

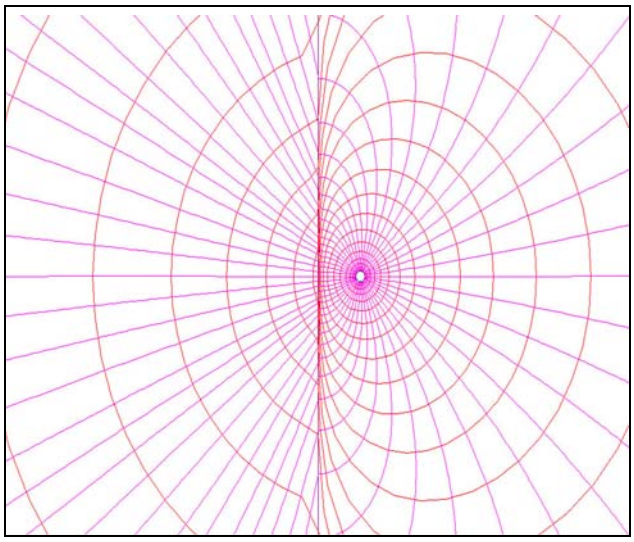

Fig. 3c. **This example shows the distribution of the electric field strength lines of RF ablation crossing through the border between two environments**

One of the more important possible assumptions made from these theoretical calculations is that the concentration of the ablating electrode cooling solution may lead to the situation when the average area of tissue damage will be smaller although the tissue heating temperature is bigger. These theoretical assumptions affirm the results of our experiments. In our experiments, we found that when the tissue ablation is performed with lower concentrations of NaCl cooling solutions, tissue damage intensity was higher and the average area of lesion was smaller in comparison with the cases when higher concentrations of NaCl cooling solutions were used. Thereby we think that this effect results in relation to the redistribution of electric field strength lines of RF ablation in tissues and cooling solution around ablating electrode concerning different concentrations of solution.

Conclusions. 1) Our experimental results show that, the maximum average temperature on the surface of the heated tissues at the electrode contact site during the ablation procedure was in the NC experimental session, when RF ablation was performed without ablation electrode cooling. When the cooling of ablation electrode was performed using the 0.1% NaCl solution, the average temperature on the tissue surface was 0.6-6 ºC lower than in the NC experimental session ($p<0.05$). The lowest average temperature on the surface of the heated tissues at the electrode contact site was determined when the ablation electrode was cooled with 0.9% NaCl solution. In this C0.9 experimental session, the average temperature was by 5.6–12 ºC lower compared to the results obtained in the NC experimental session ($p<0.05$).

2) Comparing the experimental results among all experimental sessions we determined that the impact of RF ablation on tissue damage character was the highest in the NC experimental session and the lowest in the C0.9 experimental session.

3) After RF ablation procedure, the average damage area of heated tissue was the highest in the NC experimental session. In the C0.1 experimental session, the average damage area of tissue damage was much smaller as compared with the results obtained in C0.9 and NC experimental sessions ($p<0.05$). In the C0.9 experimental session, the average area of tissue damage was smaller than in the NC experimental session but higher than C0.1 experimental session ($p<0.05$).

4) Experimental results and theoretical calculations allowed making an assumption, that the concentration of NaCl cooling solution can influence the average size and the character of the ablated tissue damage.

5) Examination of histological preparations revealed that after cooling ablation in the heated tissues the enclosed „ring“-shape stripe of damaged area appears. This damage consists of small autolyzed fibre fragments. It was also determined, that the damage of fibres presented inside and outside the „ring“ shape stripe in some of the cases is less expressed as compared to the damage of fibres presented directly in the „ring“ or in place which coincide with the ablation electrode contact site.

Referentes

1. Bhavaraju N.C., Valvano J.W. Thermophysical properties of swine myocardium. Int J Thermophys, 1999. V. 20. P. 665–666.

2. Bunch T.J., Asirvatham S.J., Friedman P.A., Monahan K.H., Munger T.M., Rea R.F., et al. Outcomes after cardiac perforation during radiofrequency ablation of the atrium. J Cardiovasc Electrophysiol, 2005. V. 16. P. 1172–1179.

3. Calkins H., Reynolds M.R., Spector P., Sondhi M., Xu Y., Martin A., et al. Treatment of atrial fibrillation with anti-arrhythmic drugs or radio frequency ablation: Two systematic literature reviews and meta-analyses. Circ Arrhythm Electrophysiol, 2009. V. 2. P. 349–361.

4. Cerecedo D., González S., Mondragón M., Reyes E., Mondragón R. In - vitro model for the ultrastructural study of the formation of thrombi in human platelets. Blood Coagul Fibrinolysis, 2006. V. 17. P. 161–164.

5. Cosman E.R., Rittman W.J., Nashold B.S., Makachinas T.T. Radiofrequency lesion generation and its effect on tissue impedance. Appl Neurophysiol, 1988. V. 51. P. 230–242.

6. Filho C.A., Lisboa L.A.F., Dallan L.A.O., Spina G.S., Grinberg M., Scanavacca M., et al. Effectiveness of the Maze procedure using cooled - tip radiofrequency ablation in patients with permanent atrial fibrillation and rheumatic mitral valve disease. Circulation, 2005. V. 112. P. I–20–I–25.

7. Güden M., Akpinar B., Sanisoğlu I., Sağbaş E., Bayindir O. Intraoperative saline - irrigated radiofrequency modified Maze procedure for atrial fibrillation. Ann Thorac Surg, 2002. V. 74. P. S1301–S1306.

8. Jongbloed M.R.M., Kelder T.P., Den Uijl D.W., Bartelings M.M., Molhoek S.G., Tukkie R., et al. Anatomical perspective on radiofrequency abatidon of AV nodal reentry tachycardia after Mustard correction for transposition of the great arteries. PACE., 2010. doi:10.1111/j.1540–8159.2010.02928.x

9. Moulton L. Cooled tip catheter ablation. EP lab digest, 2003. V. 3. P. 8–11.

10. Nakagawa H., Yamanashi W.S., Pitha J.V., Arruda M., Wang X., Ohtomo K., et al. Comparison of in vivo tissue temperature profile and lesion geometry for radiofrequency ablation with a saline - irrigated electrode versus temperature control in a canine thigh muscle preparation. Circulation, 1995. V. 91. P. 2264–2273.

11. Nakagawa H., Wittkampf F.H., Yamanashi W.S., Pitha J.V., Imai S., Campbell B., et al. Inverse relationship between electrode size and lesion size during radiofrequency ablation with active electrode cooling. Circulation, 1998. V. 98. P. 458–465.

12. Nattel S. Experimental evidence for proarrhythmic mechanisms of antiarrhythmic drugs. Cardiovasc Res, 1998. V. 37. P. 567–577.

13. Nattel S. New ideas about atrial fibrillation 50 years on. Nature, 2002. V. 415. P. 219–226.

14. Organ L.W. Electrophysiologic principles of radiofrequency lesion making. Appl Neurophysiol, 1976-1977. 39, 69–76.

15. Oral H., Chugh A., Good E., Wimmer A., Dey S., Gadeela N., et al. Radiofrequency catheter ablation of chronic atrial fibrillation guided by complex electrograms. Circulation, 2007. V. 115. P. 2606–2612.

16. Petersen H.H., Chen X., Pietersen A., Svendsen J.H., Haunso S. Lesion dimensions during temperature - controlled radiofrequency catheter ablation of left ventricular porcine myocardium: impact of ablation site, electrode size, and convective cooling. Circulation, 1999. V. 99. P. 319–325.

17. Petersen H.H., Roman – Gonzalez J., Johnson S.B., Svendsen H.J., Hauns O.S., Packer D.L. Mechanisms for enlarging lesion size during irrigated tip radiofrequency ablation: is there a virtual electrode effect?. J Interv Cardiol, 2004. V. 17. P. 171–177.

18. Stagegaard N., Petersen H.H., Chen X., Svendsen J.H. Indication of the radiofrequency induced lesion size by pre - ablation measurements. Europace, 2005. V. 7. P. 525–534.

19. Ware D.L., Boor P., Yang C., Gowda A., Grady J.J., Motamedi M. Slow intramural heating with diffused laser light: A unique method for deep myocardial coagulation. Circulation, 1999. V. 99. P. 1630–1636.

20. Weiss C., Srewart M., Franzen O., Rostocck T., Becker J., Skarda J,R. et al. Transmembraneous irrigation of multipolar radiofrequency ablation catheters: Induction of linear lesions encircling the pulmonary vein ostium without the risk of coagulum formation? Journal of Interventional Cardiac Electrophysiology, 2004. V. 10. P. 199–209.

21. Wittkampf F.H., Nakagawa H., Yamanashi W.S., Imai S., Jackman W.M. Thermal latency in radiofrequency ablation. Circulation, 1996. V. 93. P. 1083–1086.

22. Yokoyama K., Nakagawa H., Wittkampf F.H.M., Pitha J.V., Lazzara R., Jackman W.M. Comparison of electrode cooling between internal and open irrigation in radiofrequency ablation lesion depth and incidence of thrombus and steam pop. Circulation, 2006. V. 113. P. 11–19.

23. Tatur, T.A. Osnovi teoriji elektromagnitnogo polia. Moskva, Vissaja skola, 1989. P. 212–215.

24. Tungjitkusolmun S., Woo E.J., Cao H., Tsai J.Z., Vorperian V.R., Webster J.G. Thermal - electrical finite element modelling for radio frequency cardiac ablation: effects of changes in myocardial properties. Med Biol Eng Comput, 2000. V. 38. P. 562–568.

Received 10 October 2011
Accepted 21 September 2012